Ceramics-Silikáty 63 (2), 174-184 (2019)
www.ceramics-silikaty.cz doi: 10.13168/cs.2019.0009

PROPERTIES AND MICRO-STRUCTURE ASSESSMENT OF BUILDING MATERIALS BASED ON FLUE GAS DESULFURISATION GYPSUM MODIFIED BY CEMENT AND INDUSTRIAL WASTE

LEI YANG*, #MIN JING**, ***, LINGCHAO LU*, XIANTAO SONG***, XIAOBIN DONG***

*School of Materials Science and Engineering, University of Jinan, Jinan 250022, China
**Shandong Co-Innovation Center of Green Building, Shandong Jianzhu University, Jinan 250101, China
***School of Materials Science and Engineering, Shandong Jianzhu University, Jinan 250101, China

#E-mail: shandajingm@163.com

Submitted November 14, 2018; accepted February 15, 2019

Keywords: Activators, Orthogonal test, Industrial waste, Periodical-soaking

Utilisation and recycling of industrial waste and by-products to prepare building materials is the green style and contributes to the resource conservation and environmental protection. In this paper, the orthogonal test and two curing methods including 7-day non-soaking curing and 28-day periodical-soaking curing are used to investigate the effect of cement, activators and waste like blast furnace slag, silica fume and fly ash on the properties of FGD gypsum-based composites. Three typical specimens from the orthogonal test are chosen, a pure gypsum specimen, a specimen with prominent combination properties and a specimen with a big fall in strength after the 28-day periodical-soaking curing, to explore their composition and structure characterisation in two curing methods by XRD, SEM-EDS and DTA-TG. It was found that the properties of the composites, especially the waterproof property, can be improved by adding an appropriate amount of OPC and waste due to the synergistic effect between them. The periodical-soaking curing accelerates the hydration of the active substances in the composites, which promotes forming more C–S–H gel, AFt crystals or tacharanite. After the 28-day periodical-soaking, the flexural and compressive softening coefficient are 79.8 % and 107.8 % higher than that of 28-day pure FGD gypsum specimens, respectively. However, improper composition can produce excessive ettringite, which can damage the mechanical properties and water resistance of the specimens due to the expansibility of ettringite.

INTRODUCTION

The development of industrial activities such as steel and iron manufacturing, smelt and power generation lead to the release of large quantities of flue gas desulfurisation (FGD) gypsum [1], blast furnace slag (BFS) [2], silica fume (SF) [3], and fly ash (FA) [4], which occupies much land and poses a threat to the environment if disposed in landfills. Therefore, it is a hot topic to use and recycle these industrial wastes instead of landfilling [5-8].

FGD gypsum is a by-product of power station where FGD equipment is installed to remove SO_2 from the flue gas by adding limestone/lime. The higher content of calcium sulphate dihydrate, fewer impurities, smaller and more uniform particle size, wider range of sources, better fire resistance, lower thermal expansion coefficient, lower cost and sounder insulation properties are the obvious advantages of FGD gypsum [1, 9-11]. It is applied widely in construction and building engineering materials nowadays, for example, as a cement-coagulation agent or raw material in the production of cement and concrete to control the hydration rate of cement and improve the early strength, or as a body of cementitious materials after calcined to prepare lightweight gypsum-based building elements [12-14]. The latter, appearing in the form of gypsum-based blocks, gypsum particleboards or gypsum plasterboards, is a better way to reuse or recycle, as far as the consumption quantity of FGD gypsum waste [15-17]. However, the fact that is not desirable in the FGD building gypsum is the kind of air-hardening of the binding materials which are commonly used indoor because of its low mechanical strength, high solubility and poor resistance to water [18, 19].

FA, BFS and SF are by-products from coal burning thermal power stations, manufacturing of pig iron and the electrometallurgy industry, respectively [2, 3, 4, 20, 21]. Due to their good pozzolan and water-hardening nature, they are usually utilised in the manufacturing of cement and concrete, which has a low post-performance loss [22-24]. For example, Naishu et al. [25] investigated when the silica fume is migrated from the cement matrix and diffused to the concrete interface to form amounts of hydration products. So, some researchers attempted to add one or two of them into gypsum to improve the partial properties of the gypsum and explored the hydrate mechanism of these gypsum-based mixtures by SEM, XRD or DSC [13, 26, 27] in the meantime.

Zhao et al. [19] utilised FGD gypsum, granulated blast-furnace slag and high calcium fly ash to prepare water resistant blocks, finding that the softening coefficient of the product prepared is over 0.80 after the curing temperature of 60 °C and curing time of 16 h due to the formation of ettringite (AFt). Ettringite is a compound characterised by satisfactory mechanical strength, water insolubility and fire resistance [28]. Antonio et al. [13] investigated the hydration ternary systems consisting of 40 % FGD gypsum, 35 % calcium hydroxide and 25 % fly ash, presenting that the samples have better mechanical properties and water resistance at curing temperatures up to 85 °C for 7 days because of the combined action of AFt and C–S–H. But AFt is responsible for an expansive behaviour, which will reduce the properties of the material if it contains too much. Generally speaking, the curing age of the gypsum products is generally short (within several days) even if some inorganic minerals are added. This is because gypsum can basically hydrate within hours. However, those water-hardening materials have two characteristics of curing, one is that the curing period is longer; the other is that water or alkaline environment will make the hardening get better. Hence, Zhao et al. [19] found that there are still some obviously non-hydrated components, such as silicon dioxide, in the composite system. In addition, even at an extended age (increased to 28 days), the active components of the inorganic minerals react slowly due to the insufficient amount of water or activators [29]. Therefore, the selection of the composition and curing method of the specimens are very important. It is perfect if a sufficient amount of water and a kind of alkaline environment is given to the gypsum-based composites during the curing, then the water-hardening materials added in the system can be fully hydrated.

On the basis of the above-mentioned considerations, we are going to adopt a new curing method, which is called the 28-day periodical-soaking curing. It is different from the normal curing method of gypsum and includes 7 days of air curing and a subsequent 3 cycles, each cycle including 2 hours soaking curing in an alkaline solution and 166 hours of air curing. The 2-hour soaking in an alkaline solution in every cycle makes the blocks obtain the necessary water and prevents the loss of the internal activator and accelerates the hydration of the non-hydrated active substances in the composites. Meanwhile, the structure of gypsum does not subject a lot of damage over a short soaking time of only 2 hours. In this paper, we carry out the experiment on comparing the FGD gypsum-based specimens that experienced the 28-day periodical-soaking curing with those that experienced the 7-day non-soaking air curing in their micro-structure and the properties including compression strength, flexural strength and water-resistance. Before this experiment, the orthogonal test with five variables of OPC, FA, BFS, SF and activators are conducted to prepare our target specimens with the appropriate amounts of waste BFS, FA and SF. It is assured that every sample consists of more than 90 % waste. The hydration mechanism, the synergistic effect between the inorganic minerals and its performance characteristics after the 28-day periodical-soaking curing are investigated in detail.

EXPERIMENTAL

Raw materials

The FGD gypsum used in this work was from the power station in Zibo (China) and was calcined into FGD building gypsum with a standard consistency of 57 %, an initial setting time of 9.5 min, and a final setting time of 13 min, by Zibo Lvneng Building Materials Corporation (China). The OPC (42.5 grade), fly ash (FA), blast furnace slag (BFS) and silica fume (SF) were also produced in China. The detailed chemical constituents of these raw materials are shown in Table 1. The Sodium citrate, calcium chloride and calcium hydrate were all made at the Sinopharm Group (China) and the activators were prepared by calcium chloride and calcium hydrate. Figure 1 shows the XRD analysis of the FGD building gypsum from industrial calcining, which indicated that the building gypsum mainly consisted of β-hemihydrate ($CaSO_4 \cdot 1/2H_2O$), located around 2θ of 14.7°, 30°, 31.8° and 32°. In addition, there was a small amount of anhydrite ($CaSO_4$III) located around the 2θ of 14.6°, 29.6° and 32° based on the PDF database. The particle diameter of the FGD building gypsum powders is given in Figure 2. The scanning electron microscopy (SEM) images of the various inorganic modifier materials are shown in Figure 3.

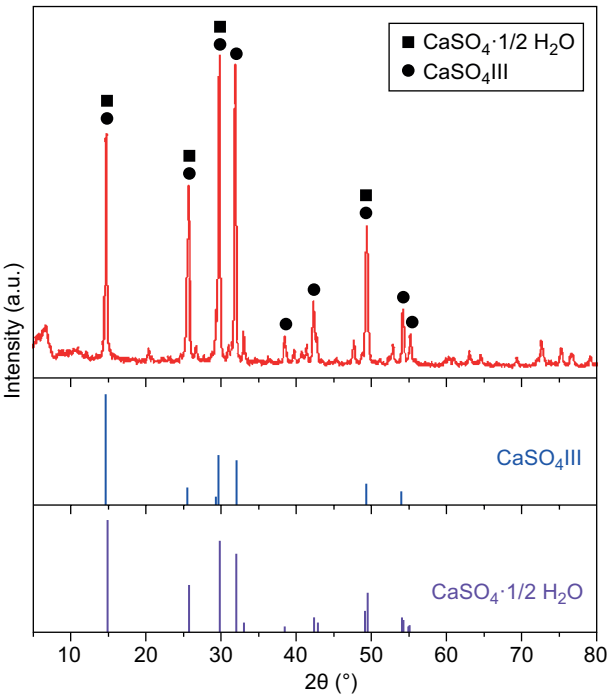

Figure 1. The XRD analysis of the FGD building gypsum.

Table 1. The detail chemical constituents of the raw materials (% by mass).

Raw material	FGD building gypsum	OPC	FA	BFS	SF
SiO_2	2.35	23.52	49.12	36.14	89.86
Al_2O_3	0.32	5.76	29.33	16.08	0.96
Fe_2O_3	0.18	2.31	6.57	0.76	1.04
CaO	39.33	61.41	8.32	32.23	0.74
SO_3	51.12	2.38	0.57	1.79	0.01
MgO	1.07	2.19	1.53	10.76	1.45
K_2O	0.08	0.12	0.13	0.02	1.02
TiO_2	0.02	0.15	0.91	0.03	0.17
LOI	4.98	1.52	2.84	0.76	3.57

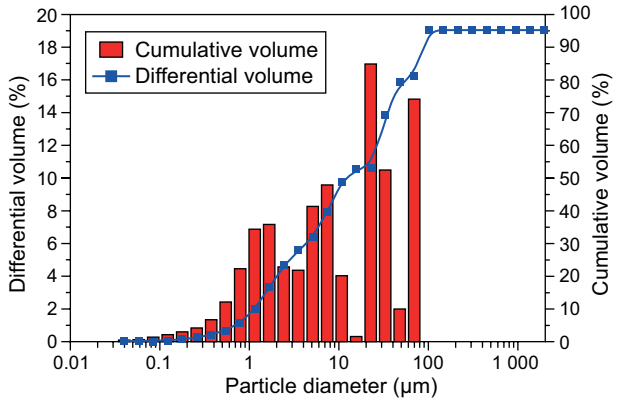

Figure 2. The particle diameter of the FGD building gypsum powders.

Orthogonal test design and sample preparation

The FGD building gypsum, sodium citrate as a retarder, the modifiers and water were mixed together. During the mixing, the proportion of the retarder sodium citrate was 5 ‰ of the FGD building gypsum and the water-binder ratio was 57 %. The dosages of the modifiers including OPC (a), FA (b), BFS (c), SF (d) and the activators (e) which can probably affect the properties of the gypsum-based blocks were designed as five elements of the orthogonal test. The factors and levels of the orthogonal test L16 (4^5) are shown in Table 2.

The detailed preparation procedures of the FGD gypsum-based building materials were as follows: The mixture above was stirred evenly by an electric mixer

Table 2. The factors and levels of the orthogonal experiment (% by mass).

Level	1	2	3	4
OPC	0	3	6	9
FA	0	3	6	9
BFS	0	4	8	12
SF	0	2	4	6
activators	0	2	4	6

Note: the percent is in the base of the weight of the FGD gypsum

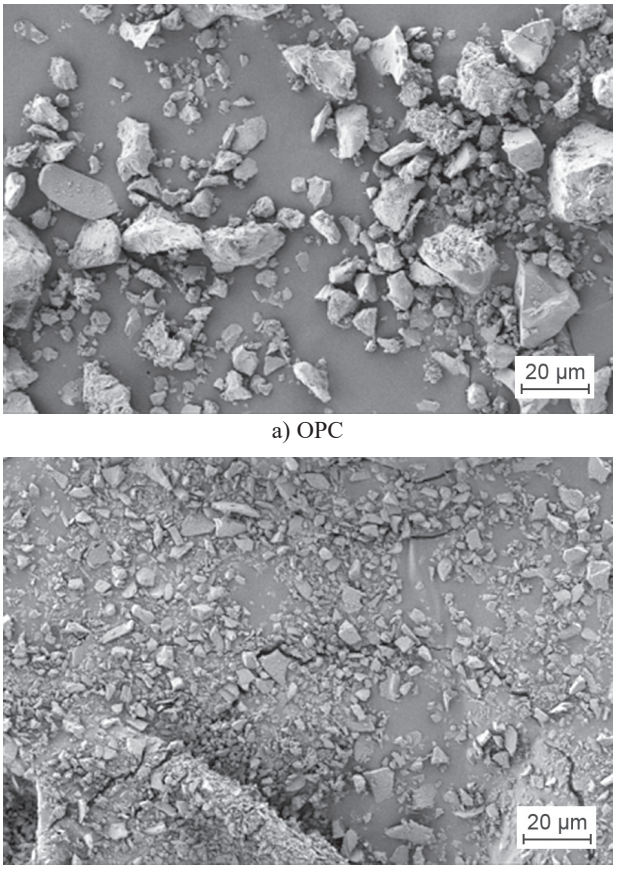

a) OPC b) FA

c) BFS d) SF

Figure 3. The SEM images of the various inorganic modifier materials: a) OPC; b) FA; c) BFS; d) SF.

and poured into a die with a size of 40 × 40 × 160 mm^3 moulds to prepare the sixteen groups of testing specimen blocks according to the orthogonal test designed, named A1-A16 in sequence. Every group of the testing specimens, including 12 blocks were evenly divided into two parts. One part was kept in an air curing environment of 20 ± 1 °C and 90 ± 1 % RH for 7 days, named the 7-day non-soaking specimens. The other blocks, after the 7-day non-soaking, they needed to experience three more of the same curing cycles during the 21 days, which were named the 28-day periodical-soaking specimens. Every curing cycle includes a 2-hour soaking in an alkaline aqueous solution (20 ± 3 °C) and a subsequent 166 hours curing at 20 ± 1 °C and 90 ± 1 % RH.

The properties tested and materials properties

After curing, half of the 7-day non-soaking specimen blocks as well as half of the 28-day periodical-soaking specimen blocks were soaked in water (20 ± 1 °C) for 24 h, and then taken out to be wiped with a wet cloth. The compression and flexural strength of these specimen blocks were tested according to the Chinese National Standard GB/T 17669.3-1999 by using a microcomputer controlled electronic pressure testing machine (CDT 1305-2 made in China), whose testing valuewas were marked as R_1. The other half of the 7-day non-soaking and 28-day periodical-soaking specimen blocks were directly dried to a constant weight at the temperature of 40 ± 2 °C and then were measured by the same electronic pressure testing machine. Their testing value of the compression and flexural strength were named the absolute dry strength, marked as R_2. The softening coefficient analyses were undertaken according to the Chinese Standard JC/T 698-2010, which was used to evaluate the water resistance of the gypsum blocks. The softening coefficient of gypsum block was calculated by Equation 1:

$$K_f = R_2/R_1 \quad (1)$$

where K_f is the softening coefficient, R_1 is the average absolute dry strength value of the dry specimens (MPa), R_2 is the average breaking load value of the water-saturated specimens (MPa).

The characterisation method

X-ray diffraction (XRD) by means of the powder method was achieved in a Bruker D8 Advance (Germany), whose date were obtained from 2θ = 10 to 60°. The surface structures were studied using a JSM-6380LA scanning electron microscopy (SEM, Japan). A differential thermal analysis (DTA) and a thermo-gravimetric (TG) using a DTU-2B thermal analyser (China) was used to quantitatively estimate the hydration phases content, from room temperature up to 800 °C, with a rate of heating of 10 °C min^{-1} in an air atmosphere.

RESULTS AND DISCUSSIONS

The mechanical properties of the 7-day non-soaking specimens and the 28-day periodical-soaking specimens

The response data obtained from the orthogonal experiments are listed in Table 3 in which A1 is the pure FGD building gypsum blocks while the others are gypsum blocks added by modifiers. The 7-day non-soaking specimen blocks are marked as 7D while the 28-day periodical-soaking specimen blocks are marked as 28D in Table 3.

Table 3. The mechanical properties of the 7-day non-soaking specimens and 28-day periodical-soaking specimens.

Group	Absolute dry strength (MPa)				Softening coefficient (K_f, 1)			
	Flexural		Compressive		Flexural		Compressive	
	7D	28D	7D	28D	7D	28D	7D	28D
A1	5.10	5.07	21.20	19.19	0.405	0.381	0.322	0.304
A2	6.35	4.86	19.51	16.86	0.534	0.645	0.495	0.532
A3	6.05	4.85	21.82	15.48	0.562	0.583	0.512	0.612
A4	5.25	5.18	20.41	18.25	0.653	0.655	0.565	0.563
A5	5.84	4.40	20.11	15.74	0.464	0.664	0.483	0.615
A6	5.20	3.77	15.72	12.97	0.461	0.653	0.494	0.495
A7	6.55	6.62	24.81	27.47	0.572	0.574	0.521	0.497
A8	7.65	5.64	24.63	23.30	0.525	0.600	0.545	0.594
A9	6.70	7.25	25.45	26.78	0.683	0.685	0.635	0.632
A10	5.95	5.24	24.05	23.58	0.645	0.654	0.463	0.478
A11	6.50	5.99	22.13	19.16	0.364	0.512	0.525	0.594
A12	7.00	5.05	22.02	17.45	0.392	0.552	0.417	0.453
A13	6.50	7.10	23.43	25.05	0.355	0.356	0.563	0.512
A14	7.25	6.50	24.31	22.27	0.287	0.299	0.414	0.483
A15	7.50	7.07	24.12	24.89	0.495	0.592	0.555	0.571
A16	6.50	4.84	18.65	17.94	0.445	0.583	0.521	0.540

For most of the specimens, the strength properties of the 28D specimens became worse than that of the 7D specimens. On the contrary, the strength properties of A7, A9 and A13 got much better after the periodical-soaking in water. However, it is a different situation for the softening coefficient. The softening coefficient of most of the specimens experiencing 28D curing is similar to or higher than those of the 7D specimens. So, it is clearly seen that the resistance to water of gypsum blocks is improved by adding the inorganic modifier.

There are two kinds of typical specimens which excite our interests in Table 3. One is the A9 specimens, both the 7D and 28D specimens, which have satisfactory combination properties. Moreover, the flexural and compression absolute dry strength of the 28D specimens increased by about 43 % and 39.5 %, respectively, comparing with that of the 28D pure FGD building gypsum specimens. Simultaneously, the flexural and compressive softening coefficient (K_f) are 79.8 % and 107.8 % higher than that of 28D pure FGD building gypsum specimens, respectively. This is because the specimen properties can be improved by the synergistic effect between the OPC and waste, which promotes forming more compactness and waterproof substances. The other is the A12 specimens which have a big fall in the strength properties after the 28D experiment. The flexural and compression absolute dry strength of the A12-28D periodical-soaking specimens reduced by 27.8 % and 20.7 %, respectively, compared to that of the A12-7D non-soaking specimens. Therefore, the micro-structure and hydrated mechanism of the A9 and A12 specimens, as well as the A1 specimens as the reference specimens, are explored and analysed in detail below.

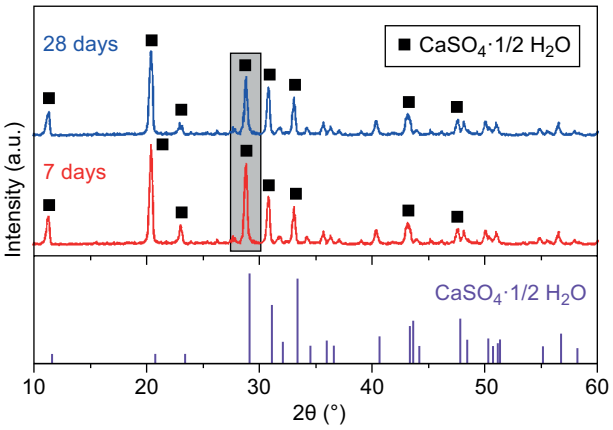

a) A1

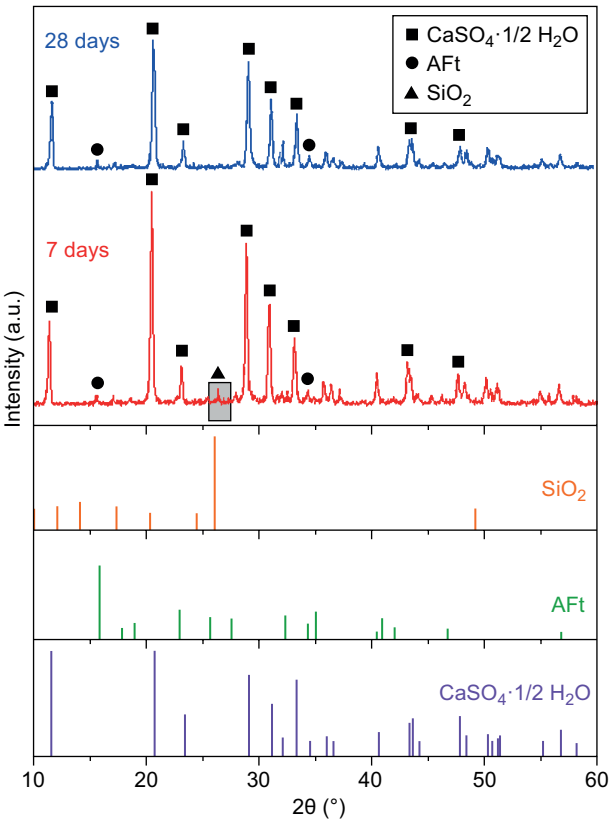

b) A9

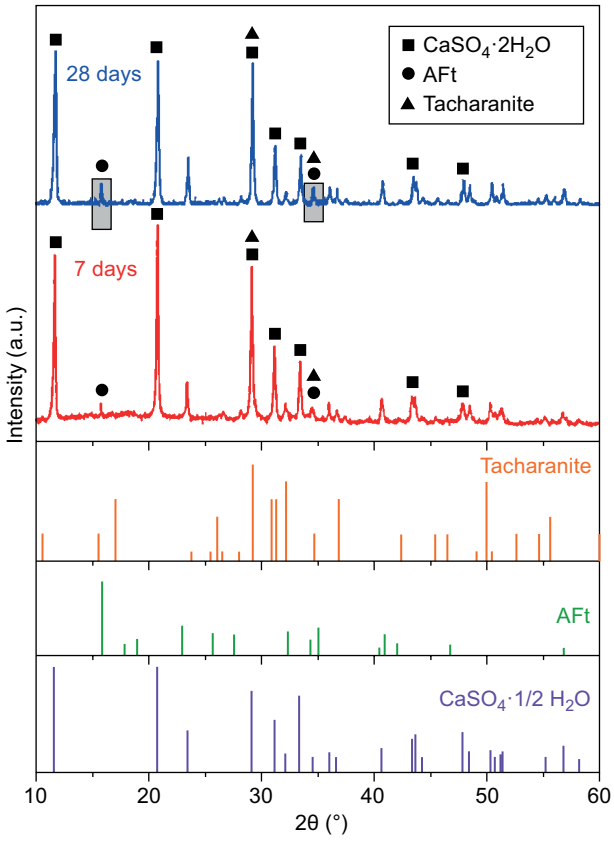

c) A12

Figure 4. The XRD correlation pattern of the 7D specimens and 28D specimens: a) A1 specimens; b) A9 specimens; c) A12 specimens.

The phase-structure of the 7-day non-soaking specimens and the 28-day periodical-soaking specimens

Figure 4 shows the XRD patterns of the A1, A9 and A12 specimens, in which it is shown that the dihydrate calcium sulfate crystal is the main hydrate product labelled as A on the diffraction peak. After the 28-day periodical-soaking curing, the diffraction peaks strength of the dihydrate calcium sulfate crystal decreased slightly not only because of the high solubility of gypsum when meeting the alkaline aqueous solution, but also owing to the crystalline transformation and fracture of the dihydrate calcium sulfate crystal in the later stages. It is demonstrated that the short-time soaking in the alkaline solution does harm the pure dihydrate calcium sulfate crystal structure.

The weak diffraction of ettringite (AFt) and SiO_2 labelled as B and C in Figure 4b of the A9-7D specimens can be obviously observed. The formation of AFt is the result of synergism by the FGD gypsum, OPC, BFS and the activators, as can be seen in the following Equation 2 and 3. But the diffraction peaks' strength of SiO_2 of the A9-28D specimens disappeared illustrating that the reactive SiO_2 has basically been completed.

$$3CaO{\cdot}Al_2O_3 + Ca(OH)_2 + H_2O \rightarrow \rightarrow xCaO{\cdot}Al_2O_3{\cdot}yH_2O \quad (2)$$

$$xCaO{\cdot}Al_2O_3{\cdot}yH_2O + CaSO_4{\cdot}2H_2O + H_2O \rightarrow \rightarrow 3CaO{\cdot}Al_2O_3{\cdot}3CaSO_4{\cdot}32H_2O\ (AFt) + + Ca(OH)_2 \quad (3)$$

Figure 4c shows that the A12 specimens generated more AFt phases and a small amount of tacharanite ($12CaO{\cdot}Al_2O_3{\cdot}18SiO_2{\cdot}18H_2O$) after the 28-day curing, compared with the sample of the 7-day in Figure 4c. More importantly, the diffraction peaks' strength of the AFt phases of the A12 specimens obviously increased after the 28-day curing due to the increased content of aluminates that are mainly derived from OPC, BFS and FA.

The micro-structure of the 7-day non-soaking specimens and the 28-day periodical-soaking specimens

The above phenomenon can be supported by SEM in Figure 5, which shows the SEM microstructural characteristics of the A1, A9 and A12 specimens. The EDS analysis results of the selected region for the specimens are shown in Figure 6 and Table 4. In Figure 5a, it can be seen that the crystal of $CaSO_4{\cdot}2H_2O$ of the A1-7D specimen presents as long columnar. However, the crystal of $CaSO_4{\cdot}2H_2O$ of the A1-28D specimen is a little thicker and packs more disorder with more porosity as shown in Figure 5b. It is caused by the partial dissolution and crystalline transformation of the $CaSO_4{\cdot}2H_2O$ crystal under the curing of periodical soaking. Meanwhile, from the EDS analysis of point 1 in Figure 6b and Table 4, the columnar substance of point 1 is shown, which is mainly composed of Ca, S and O elements, which can be identified as $CaSO_4{\cdot}2H_2O$.

Figures 5c,d, e and f show the $CaSO_4{\cdot}2H_2O$ crystal morphology of the specimens is short columnar, which is induced by the basicity of the liquid phase at the initial hydration stage of the composite cementitious materials including the cement and alkaline activators. The effectiveness of the alkaline activators for accelerating the crystal transformation of gypsum has been observed previously [30]. Furthermore, Figure 5c shows the A9-7D specimens also contain a small amount of flocculent substance (point 3) and non-hydrated minerals (point 2). However, the non-hydrated minerals are not observed in Figure 5d of A9-28D, indicating that the non-hydrated minerals have hydrated after the 28-day periodical soaking curing. In addition, the content of the flocculent substance (point 3) increases significantly in the A9-28D specimen. Importantly, taking gypsum as the matrix, EDS can be mixed with a certain amount of $CaSO_4{\cdot}2H_2O$ in any area, which should be removed in the actual characterisation of the substances. Hence, Figure 6b shows that the non-hydrated minerals (point 2) is mainly composed of Ca, O, Al and Si except for the content of $CaSO_4{\cdot}2H_2O$ (which can be identified as SS) and Figure 6c shows the flocculent substance (point 3) is mainly composed of Ca, O and Si except for the content of $CaSO_4{\cdot}2H_2O$ (which can be identified as the C–S–H gel). The C–S–H gel is the hydration reaction product of C_3S and C_2S from OPC, as can be seen in Equations 4 and 5. Meanwhile, the surface of the silica fume added into A9-7D has many unsaturated bonds and many different bond states of hydroxyl groups, which can absorb Ca^{2+} in the liquid phase and transforms the C_3S-Hn with a low Ca/Si ratio into the C–S–H gel with a high Ca/Si ratio in the existence of the reactive SiO_2 and the activators in Equation 6.

$$3CaO{\cdot}SiO_2 + H_2O \rightarrow \rightarrow xCaO{\cdot}SiO_2{\cdot}yH_2O\ (C–S–H) + Ca(OH)_2 \quad (4)$$

$$2CaO{\cdot}SiO_2 + H_2O \rightarrow \rightarrow xCaO{\cdot}SiO_2{\cdot}yH_2O\ (C–S–H) + Ca(OH)_2 \quad (5)$$

$$Ca^{2+} + OH^- + SiO_2 + H_2O \rightarrow \rightarrow xCaO{\cdot}SiO_2{\cdot}yH_2O\ (C–S–HH) \quad (6)$$

There are more acicular substances (the A9 specimens contain less) and less flocculent C–S–H appearing in both the A12-7D and A12-28D specimens as shown in Figures 5e and f. Besides, there are some non-hydrated spherical particles contained in the A12-7D specimen in Figure 5e, which are not found in the A12-28D specimen in Figure 5f. Therefore, it can be concluded that the 28-day periodical-soaking curing can better accelerate the hydration reaction.

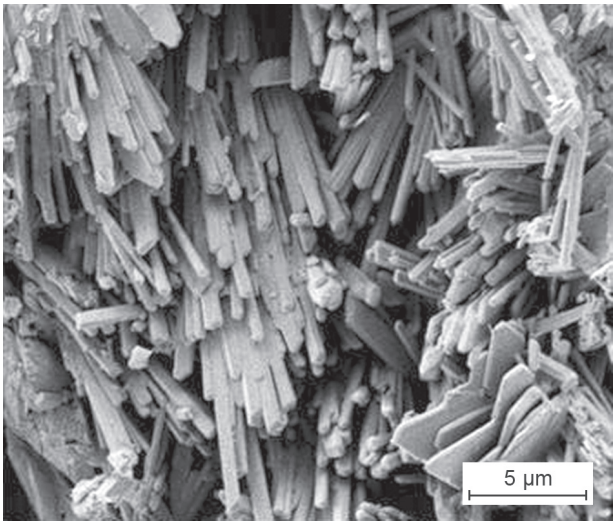

a) A1, 7 days

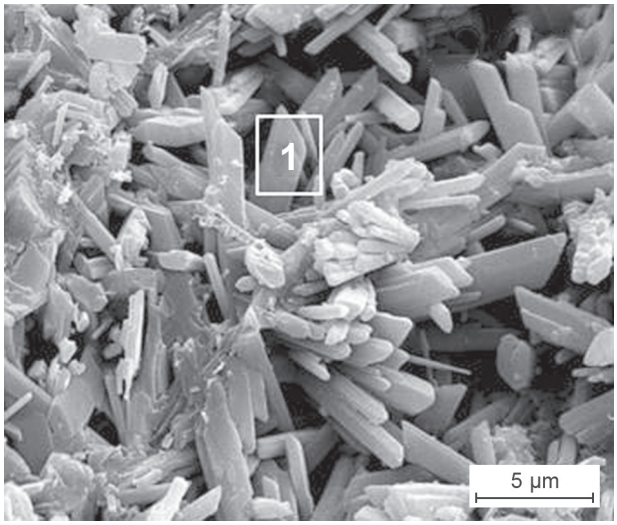

b) A1, 28 days

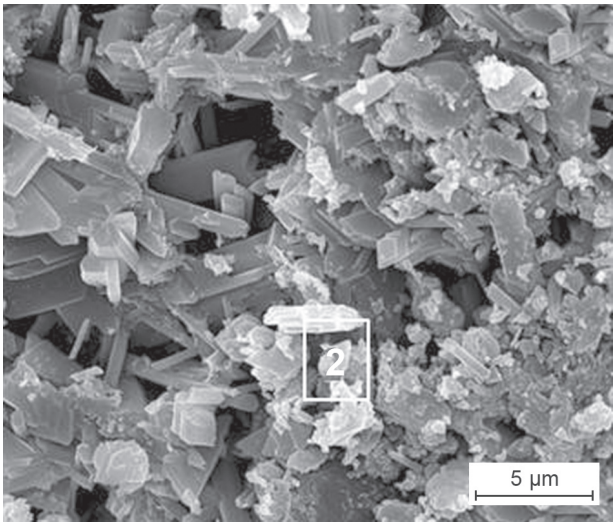

c) A9, 7 days

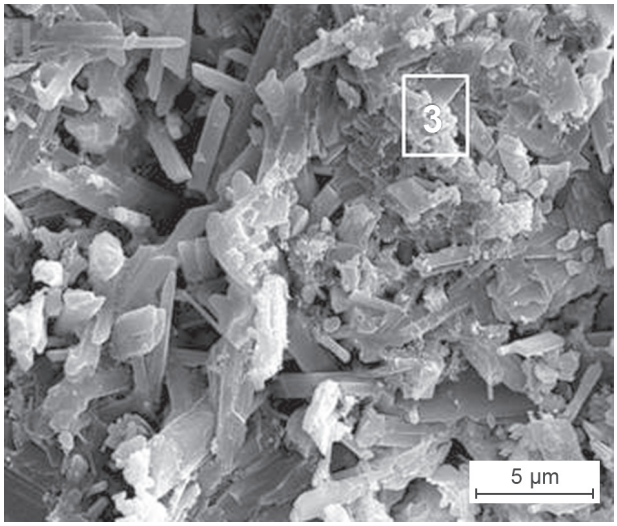

d) A9, 28 days

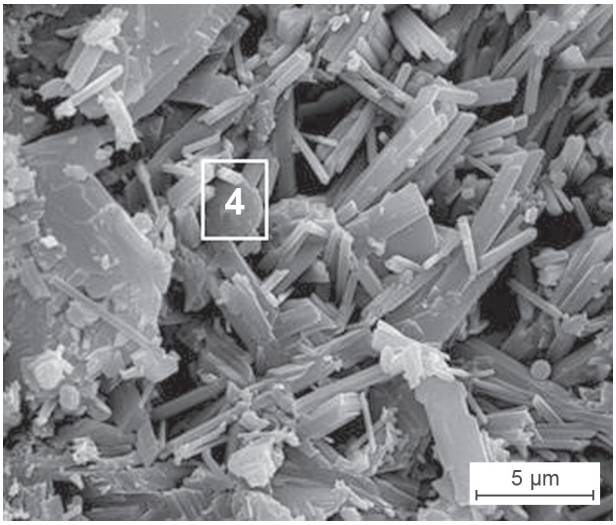

e) A12, 7 days

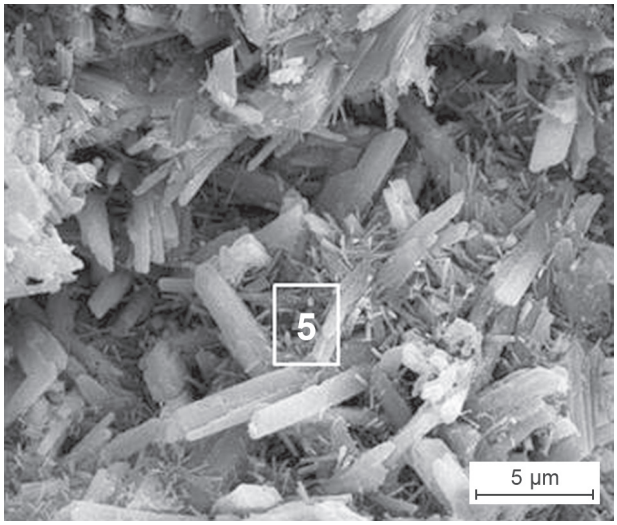

f) A12, 28 days

Figure 5. The SEM analysis of the 7-day non-soaking specimens and the 28-day periodical-soaking specimens: a), b) the A1 specimens; c), d) the A9 specimens; e), f) the A12 specimens.

Similarly, Figure 6d shows that the non-hydrated spherical particles (point 4) is mainly composed of Al, Si and Fe except for the content of $CaSO_4 \cdot 2H_2O$ (which can be identified as FA). Meanwhile, the acicular substance of point 5 in Figure 5e is composed of O, Ca, S and Al, which can be identified as AFt. But AFt is responsible for an expansive behaviour, which will reduce the properties of the material if it contains too much. This is the reason for the strength properties degradation of the A12-28D specimen. Furthermore, the A9-28D specimens show the centralised distribution of C–S–H whereas the A12-28D specimens show the uniform distribution of the AFt crystals in the system. This is because the SF is migrated from the gaps of the gypsum crystals and diffused to the gypsum-based composites interface whereas the forming of AFt has no property of migration. Hence, it is easy to form flocculent C–S–H gel on the surface of the composites and it presents as a centralised distribution characteristic.

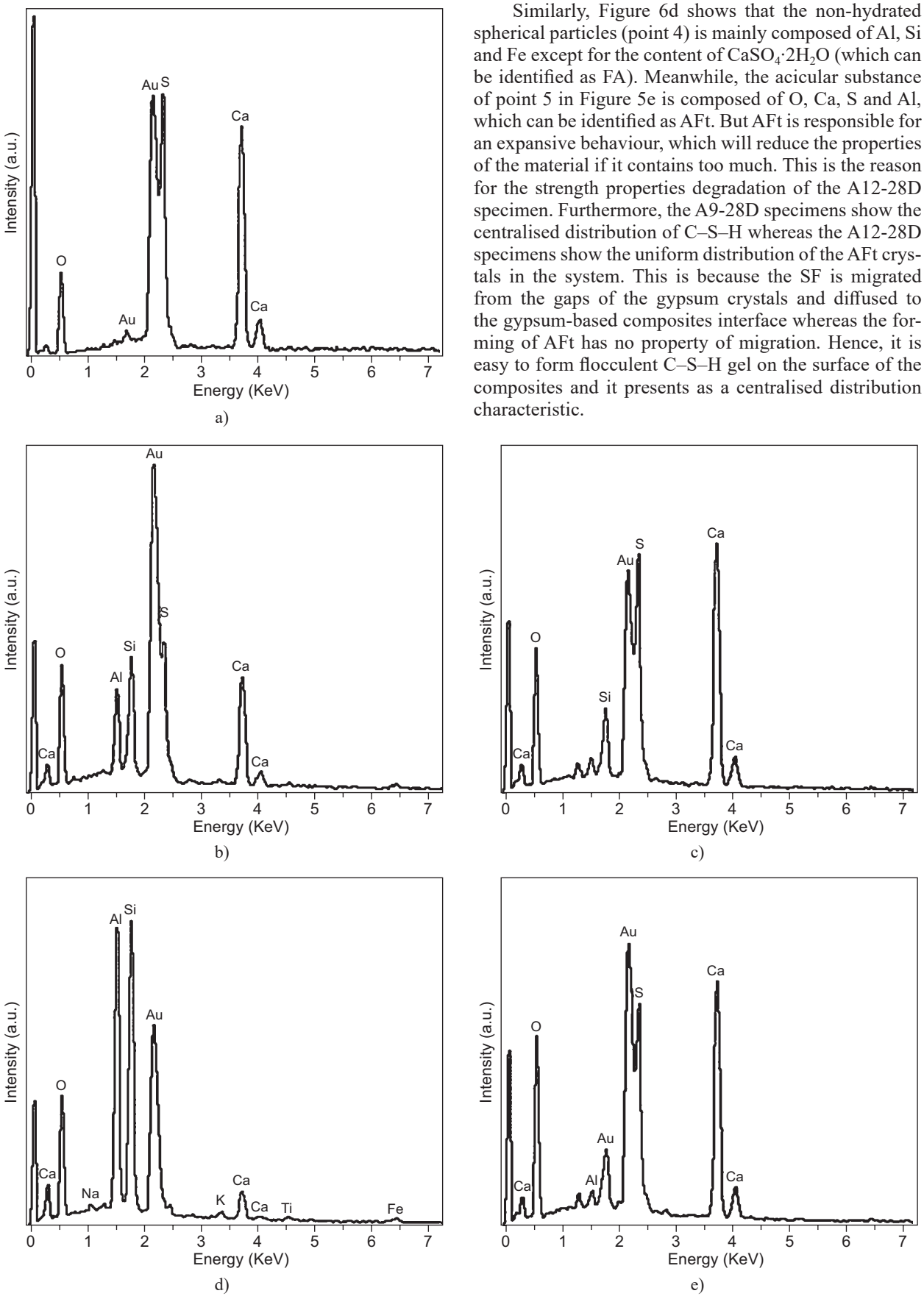

Figure 6. The EDS analysis results of the selected points: a) the EDS analysis of point 1; b) the EDS analysis of point 2; c) the EDS analysis of point 3; d) the EDS analysis of point 4; e) the EDS analysis of point 5.

Table 4. The EDS analysis results of the selected points (% by mass).

Content	O	S	Na	Al	Si	K	Ca	Ti	Fe
1	51.75	16.87	–	–	–	–	31.38	–	–
2	58.83	5.91	–	8.02	9.95	–	17.29	–	–
3	57.40	12.30	–	–	3.74	–	26.56	–	–
4	44.65	–	0.73	20.88	27.04	0.69	3.98	0.64	1.39
5	64.88	9.52	–	1.21	–	–	24.39	–	–

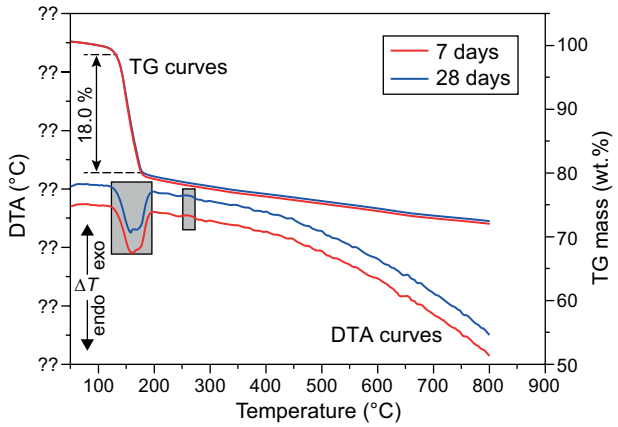

a) A1

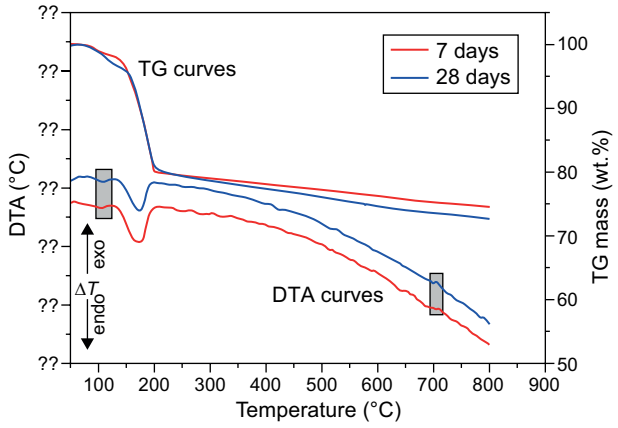

b) A9

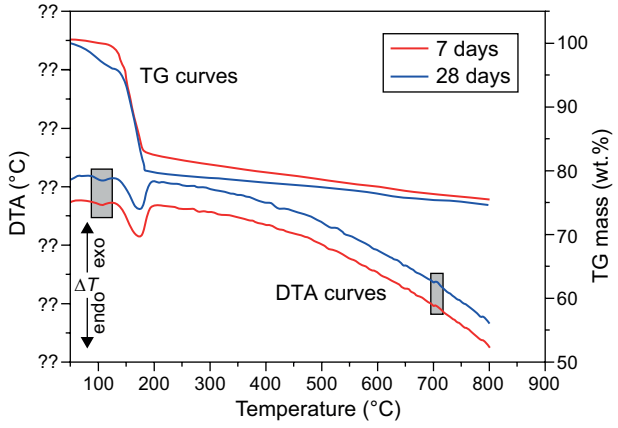

c) A12

Figure 7. The DTA-TG analysis of the 7-day non-soaking specimens and the 28-day periodical-soaking specimens: a) the A1 specimens; b) the A9 specimens; c) the A12 specimens.

The thermo-analysis of the 7-day non-soaking specimens and the 28-day periodical-soaking specimens

Figure 7 presents the DTA-TG curves of the specimens under different curing ages and curing methods. As can be seen from Figure 7a, the formation of endotherms at 126-176 °C corresponding to about 18 % mass loss in its TG curve is mainly due to the dehydration of two crystals in the water of the dihydrate gypsum. Besides sulfate calcium dihydrate, there are no other phases in the A1-7D or A1-28D specimens, so their DTA or TG curves are extremely similar.

However, it is another thing for the thermal curves of A9 and A12. There is an AFt phase or a C–S–H ($xCaO{\cdot}SiO_2{\cdot}yH_2O$) gel phase forming in the A9 and A12 specimens, which bring an obviously endothermic peak within 87-120 °C and a weak endothermic peak at about 700 °C.

Moreover, the A9-28D specimens have stronger endotherms in the DTA curve and more mass loss in the TG curve than A9-7D at 87-120 °C. It is observed more obviously when contrasting with A12-7D and A12-28D. It is demonstrated that the 28D specimens produce more AFt crystals or C–S–H gel than the 7D specimens, which is in accordance with their XRD results. The endothermic peak at 700 °C is probably mainly caused by the decomposition of the C–S–H gel. The thermo-analysis characteristic is consistent with the XRD and SEM-EDS results.

CONCLUSIONS

This experimental research investigates the effects of solid waste like BFS, SF, FA on the properties and microstructure of FGD gypsum-based composites. Based on the testing results, the following detailed conclusions can be drawn:

- The orthogonal presents that the mechanical properties and water-resistance of FGD gypsum-based composites can be improved by adding OPC and waste according to the synergistic effect between them.
- After the 28-day periodical-soaking curing, the flexural and compressive absolute dry strength of the optimal formula are increased by 43 % and 39.5 % compared with that of pure FGD gypsum, respectively.

Furthermore, the flexural and compressive softening coefficient are 79.8 % and 107.8 % higher than that of 28-day pure FGD gypsum specimens, respectively.

- The curing of the periodical soaking can make the gypsum crystal partially dissolve and make the crystal transform, which explains the performance deterioration of the pure gypsum after the 28-day periodical-soaking curing.
- The 28-day periodical-soaking curing can accelerate the hydration of the active substances of the FGD gypsum-based composites, which promotes forming more C–S–H gel, AFt crystals or tacharanite. The C–S–H gel can cover the surface of the gypsum crystals, which contributes to the inhibition of dissolution and crystal transformation of the FGD gypsum. Meanwhile, the appropriate AFt can improve the properties of the composites whereas more AFt makes the property deteriorate.

Acknowledgments

This research was supported by the Project of Shandong Province Higher Educational Science and Technology Programme (Grant No. J14LA05)

REFERENCES

1. Koralegedara N. H., Al-Abed S. R., Rodrigo S. K., Karna R. R., Scheckel K. G., Dionysiou D. D. (2017): Alterations of lead speciation by sulfate from addition of flue gas desulfurization gypsum (FGDG) in two contaminated soils. *The Science of the total environment*, 575, 1522-1529. doi: 10.1016/j.scitotenv.2016.10.027
2. Phummiphan I., Horpibulsuk S., Rachan R., Arulrajah A., Shen S. L., Chindaprasirt P. (2018): High calcium fly ash geopolymer stabilized lateritic soil and granulated blast furnace slag blends as a pavement base material. *Journal of Hazardous Materials*, 341, 257-267. doi: 10.1016/j.jhazmat.2017.07.067
3. Soliman N. A., Tagnit-Hamou A. (2017): Partial substitution of silica fume with fine glass powder in UHPC: Filling the micro gap. *Construction and Building Materials*, 139, 374-383. doi: 10.1016/j.conbuildmat.2017.02.084
4. Nath P., Sarker P. K. (2017): Flexural strength and elastic modulus of ambient-cured blended low-calcium fly ash geopolymer concrete. *Construction and Building Materials*, 130, 22-31. doi: 10.1016/j.conbuildmat.2016.11.034
5. Colangelo F., Messina F., Di Palma L., Cioffi R. (2017): Recycling of non-metallic automotive shredder residues and coal fly-ash in cold-bonded aggregates for sustainable concrete. *Composites Part B*, 116, 46-52. doi: 10.1016/j.compositesb.2017.02.004
6. Chen M., Wang S., Lu L., Zhao P., Gong C. (2016): Effect of matrix components with low thermal conductivity and density on performances of cement-EPS/VM insulation mortar. *Journal of Thermal Analysis and Calorimetry*, 126(3), 1123-1132. doi: 10.1007/s10973-016-5718-x
7. Liu C., Zhao Q., Wang Y., Shi P., Jiang M. (2016): Surface modification of calcium sulfate whisker prepared from flue gas desulfurization gypsum. *Applied Surface Science*, 360, 263-269. doi: 10.1016/j.apsusc.2015.11.032
8. Nan J., Chen X., Wang X., Lashari M. S., Wang Y., Guo Z., Du Z. (2016): Effects of applying flue gas desulfurization gypsum and humic acid on soil physicochemical properties and rapeseed yield of a saline-sodic cropland in the eastern coastal area of China. J. *Journal of Soils and Sediments*, 16(1), 38-50. doi: 10.1007/s11368-015-1186-3
9. Tesárek P., Drchalová J., Kolísko J., Rovnaníková P., Černý R. (2007): Flue gas desulfurization gypsum: Study of basic mechanical, hydric and thermal properties. *Construction and Building Materials*, 21(7), 1500-1509. doi: 10.1016/j.conbuildmat.2006.05.009
10. Wu H., Chao S., Zhou T., Liu Y. (2018): Cold-formed steel framing walls with infilled lightweight FGD gypsum Part II: Axial compression tests. *Thin-Walled Structures,* 132, 771-782. doi: 10.1016/j.tws.2018.06.034
11. Zhao S., Duan Y., Lu J., Gupta R., Pudasainee D., Liu S., Liu M., Lu J. (2018): Thermal stability, chemical speciation and leaching characteristics of hazardous trace elements in FGD gypsum from coal-fired power plants. *Fuel*, 231, 94-100. doi: 10.1016/j.fuel.2018.05.067
12. Caillahua M. C., Moura F. J. (2018): Technical feasibility for use of FGD gypsum as an additive setting time retarder for Portland cement. *Journal of Materials Research and Technology*, 7(2), 190-197. doi: 10.1016/j.jmrt.2017.08.005
13. Telesca A., Marroccoli M., Calabrese D., Valenti G. L., Montagnaro F. (2013): Flue gas desulfurization gypsum and coal fly ash as basic components of prefabricated building materials. *Waste Management*, 33(3), 628-633. doi: 10.1016/j.wasman.2012.10.022
14. Xu L., Wu K., Li N., Zhou X., Wang P. (2017): Utilization of flue gas desulfurization gypsum for producing calcium sulfoaluminate cement. *Journal of Cleaner Production*, 161, 803-811. doi: 10.1016/j.jclepro.2017.05.055
15. Anthony D. A., Mahen M. (2017): Fire tests of non-load bearing light gauge steel frame walls lined with calcium silicate boards and gypsum plasterboards. *Thin-Walled Structures*, 115, 86-99. doi: 10.1016/j.tws.2017.02.005
16. Rangavar H., Khosro S. K., Payan M. H., Soltani A. (2014): Study on the Possibility of Using Vine Stalk Waste (Vitis Vinifera) for Producing Gypsum Particleboards. *Mechanics of Composite Materials*, 50(4), 501-508. doi: 10.1007/s11029-014-9436-9
17. Li Y. Q., Yu H. Y., Qu L., Wang L. (2018): Effect of aluminum powder and NaOH on the physical and mechanical properties of aerated block with desulfurized gypsum. *Ferroelectrics*, 529(1), 59-66. doi: 10.1080/00150193.2018.1448609
18. Flores Medina N., Hernández-Olivares F., Arroyo X., Aguilera A., Fernandez F. (2016): Characterization of a more sustainable cement produced with recycled drywalland plasterboards as set retarders. *Construction and Building Materials*, 124, 982-991. doi: 10.1016/j.conbuildmat. 2016.08.140
19. Zhao F.-Q., Liu H.-J., Hao L.-X., Li Q. (2012): Water resistant block from desulfurization gypsum. *Construction and Building Materials*. 27(1), 531-533. doi: 10.1016/j.conbuildmat.2011.07.011
20. Mo K. H., Chin T. S., Alengaram U. J., Jumaat M. Z. (2016): Material and structural properties of waste-oil palm shell concrete incorporating ground granulated blast-furnace slag reinforced with low-volume steel fibres. *Journal of*

Cleaner Production, 133, 414-426. doi: 10.1016/j.jclepro.2016.05.162

21. Mobili A., Belli A., Giosuè C., Bellezze T., Tittarelli F. (2016): Metakaolin and fly ash alkali-activated mortars compared with cementitious mortars at the same strength class. *Cement and Concrete Research*, 88, 198-210. doi: 10.1016/j.cemconres.2016.07.004
22. Arulrajah A., Mohammadinia A., Phummiphan I., Horpibulsuk S., Samingthong W. (2016): Stabilization of Recycled Demolition Aggregates by Geopolymers comprising Calcium Carbide Residue, Fly Ash and Slag precursors. *Construction and Building Materials*, 114, 864-873. doi: 10.1016/j.conbuildmat.2016.03.150
23. Huang X., Wang Z., Liu Y., Hu W., Ni W. (2016): On the use of blast furnace slag and steel slag in the preparation of green artificial reef concrete. *Construction and Building Materials*, 112, 241-246. doi: 10.1016/j.conbuildmat.2016.02.088
24. Rafieizonooz M., Mirza J., Salim M. R., Hussin M. W., Khankhaje E. (2016): Investigation of coal bottom ash and fly ash in concrete as replacement for sand and cement. *Construction and Building Materials*, 116, 15-24. doi: 10.1016/j.conbuildmat.2016.04.080
25. Naishu Z., Fengnian J., Xinli K., Ying X., Jiannan Z., Bo W, Hao W. (2018): Interface and anti-corrosion properties of sea-sand concrete with fumed silica. *Construction and Building Materials*, 188, 1085-1091. doi: 10.1016/j.conbuildmat.2018.08.040
26. Qiao X. C., Poon C. S., Cheeseman C. (2006): Use of flue gas desulphurisation (FGD) waste and rejected fly ash in waste stabilization/solidification systems. *Waste Management*, 26, (2), 141-9. doi: 10.1016/j.wasman.2005.02.020
27. Shi Y. Z., Kun N., Jin M. Li. (2012): Properties of mortars made by uncalcined FGD gypsum-fly ash-ground granulated blast furnace slag composite binder. *Waste Management*, 32(7), 1468-1472. doi: 10.1016/j.wasman.2012.02.014
28. Palou M., Kuzielová E., Žemlička M., Novotný R., Másilko J. (2018): The effect of metakaolin upon the formation of ettringite in metakaolin–lime–gypsum ternary systems. *Journal of Thermal Analysis and Calorimetry*, 133(1), 77-86. doi: 10.1007/s10973-017-6885-0
29. Siyu D., Hongqiang L., Fangqin C., Huiping S., Hengquan Y. (2018): Investigation into the synergistic effects in hydrated gelling systems containing fly ash, desulfurization gypsum and steel slag. *Construction and Building Materials*, 187, 1113-1120. doi: 10.1016/j.conbuildmat.2018.07.241
30. Singh M., Garg M. (1995): Activation of gypsum anhydrite-slag mixtures. *Cement and Concrete Research*, 25(2), 332-338. doi: 10.1016/0008-8846(95)00018-6